SAW FEMs for GSM-Based Multi-Band Cellular Phones with Direct-Conversion Demodulation

M. Hikita+, N. Matsuura++, K. Yokoyama++, N. Shibagaki+, K. Sakiyama++
+: Central Research Lab., Hitachi Ltd. (e-mail: hikitami@crl.hitachi.co.jp) ++: Hitachi Media Ltd.

Abstract

Assuming the DC demodulation, required characteristics and new configurations for SAW FEMs were investigated. Parallel connections between SAW filters and the pin diode reduce the number of circuit elements drastically. The developed module for EGSM/DCS dual-band achieved Tx insertion losses as small as 1.0 dB and 1.2 dB, and Rx insertion losses of 3.0 dB and 3.3 dB for EGSM and DCS, respectively. 30-40 dB attenuation peculiarly required to DC demodulation up to several GHz was achieved. Multi-band FEMs such as triple-band FEM and so on were also investigated.

I. INTRODUCTION

Direct-conversion (DC) demodulation or low intermediate-frequency (IF) demodulation [1][2] have been widely investigated in multi-band cellular phones, such as 800-MHz extended global system for mobile communication (EGSM), 1.8-GHz digital cellular systems (DCS), 1.9-GHz personal communications system (PCS), etc. Authors have already published switch-type SAW antenna duplexers, sometimes called SAW front-end modules (FEMs), for both dual-band and triple-band transceivers [3][4]. They can be used with heterodyne demodulation. However, requirements peculiar to CD demodulation have not been taken into consideration. Based on the blocking characteristics and the spurious emissions required for EGSM, DCS and PCS specifications [5], we investigated configurations and required performances for multi-band FEMs to be used with DC demodulation. Radio-frequency (RF) integrated circuits (ICs) with DC demodulation generally have high spurious responses at the harmonic frequencies, so attenuation levels of over 30-40 dB from antenna port to receiver (Rx) ports are needed up to several GHz.

Rece ly, receiver-low-noise amplifiers (LNAs) not only have been included in RF-ICs but have also been operated differentially to reduce the effect of common-mode noise [1][2]. The former requires very low-loss characteristics for SAW filters in FEMs to compensate noise-figure (NF) degradation and the latter requires complete differential Rx outputs from FEMs. We achieved low-loss characteristics of Rx portions by new SAW-filter design procedures. We also realized differential outputs with small amplitude- and phase-imbalances by developing lumped-element baluns in the FEM. Moreover, we have achieved high isolation characteristics from transmitter (Tx) ports to Rx ports, making it possible to cut the number of switching pin diodes in half, compared with the conventional antenna switch modules [6][7][8]. The developed FEM has the size of 8×8×1.85mm3 and can be used with general RF-ICs using DC demodulation.

II. DIRECT-CONVERSION TRANSCEIVER FOR GSM-BASED MULTI-BAND PHONES

A. Block diagram

A block diagram of the conventional dual-band transceiver used in the EGSM and DCS systems is illustrated in Fig. 1(a). Heterodyne demodulation has been used, so inter-stage SAW filters (R2s) and an IF SAW filter are used between LNAs and Mixs and after Mixs, respectively. Up-conversion has been used to generate the Gaussian-filtered minimum-shift-keying (GMSK) [5] modulated signal. A conventional antenna-switch module is also shown in Fig. 1(a) [6][7][8]. It not only switches the transmitting and receiving states but also separates 900-MHz signals and 1.8-GHz signals via a diplexer consisting of low-pass/high-pass filters. Four switching pin diodes are used, two in the Tx portions and two in the Rx portions, as shown in Fig. 1(a).

A block diagram of our new dual-band transceiver using DC demodulation is shown in Fig. 1(b). The received signal is directly down converted to base-band in-phase and quadrature-phase demodulated signals. This demodulation eliminates the need for the inter-stage R2 filters and the IF SAW filter, and simplifies the receiver-circuit configuration [1][2]. A new FEM with SAW filters, the main focus of this paper, is also shown in the figure.

The offset-phase-lock-loop (OPLL) modulation method is now being used to generate GMSK signals as shown in Fig. 1(b), which simplifies the transmitter circuit configuration drastically [9][10]. This is because transmitter voltage-controlled oscillators (VCOs) are directly modulated by the base-band analog modulation signals from the OPLL circuit.

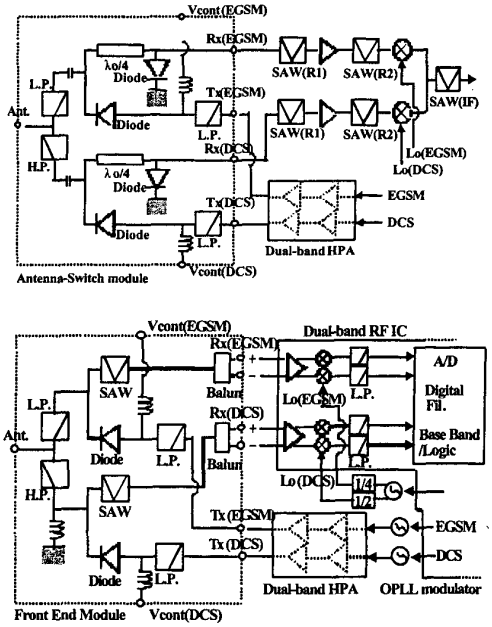

Fig. 1 Block diagram of dual-band cellular phone (EGSM and DCS). (a) Conventional heterodyne-demodulation method; antenna-switch module is used. (b) Direct-conversion demodulation method; SAW FEM is used.

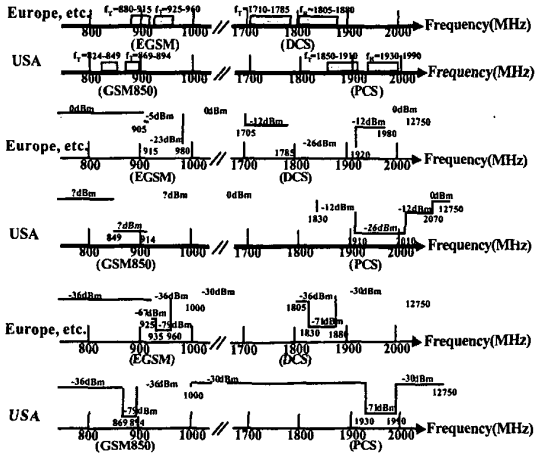

Fig. 2 System requirements for EGSM, GSM850, DCS and PCS from 3GPP regulation [5]. (a) Frequency allocations. (b) Blocking characteristics. (c) Spurious emissions.

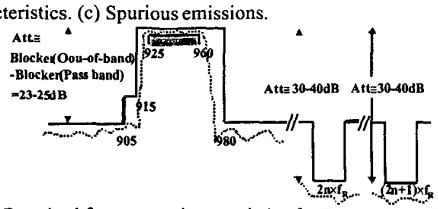

Fig. 3 Required frequency characteristics for Rx portions of FEM. Examples of EGSM are shown.

B. Requirements for receiver portions of FEM

The frequency allocations for EGSM, GSM850, DCS and PCS are shown in Fig. 2(a). The frequency responses required for the Rx portions, i.e. paths from antenna port to inputs ports of LNAs, are mainly determined by the blocking characteristics [5] shown in Fig. 2(b). RF filters are needed to protect LNAs and Mixs from these blockers. The attenuation levels in the out-of-bands are primarily determined by the difference between the blocker levels at the pass band and those at the out-of-bands. Taking EGSM as an example, these required characteristics are shown in Fig. 3.

RF-ICs with DC demodulation generally have high spurious responses at harmonic frequencies. This is because pseudo-local signals at frequencies of the local frequency multiplied by an odd-integer number are produced due to saturated operation of the 1st Mixs. Moreover, in a recent transceiver circuit, Fig. 1(b), the local signals for EGSM and DCS are generated by four- and two-time divisions, respectively, of the output signal from a single high-frequency VCO [2], which also produces pseudo-local signals at frequencies of the local frequency multiplied by an even-integer number. These pseudo-local signals convert spurious signals at harmonic frequencies into noise-like base-band signals, which are very similar to the image-frequency responses of conventional heterodyne demodulation. Therefore, SAW filters within the FEM not only suppress the blockers of Fig. 2(b) but also must have high attenuation levels of 30-40 dB at harmonic frequencies. These levels are also shown in Fig. 3.

Recently, LNAs have been included within RF-ICs. In many cases, they are operated differentially to reduce the effect of the common-mode noise within ICs [1][2]. Therefore, not only the frequency characteristics of Fig. 3 but also complete differential Rx outputs are required for the FEM .

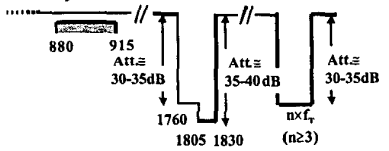

Fig. 4 Required frequency characteristics for Tx portions of FEM. EGSM are shown. 1805-1830 MHz overlaps fR(DCS).

C. Requirements for transmitter portions of FEM

Frequency responses for Tx portions, i.e. the paths from output ports of an HPA to an antenna port, are mainly determined by spurious emission characteristics [5] shown in Fig. 2(c). General HPAs have spurious emission levels of -35--40 dBc at harmonic frequencies [11]. Therefore, though pass-band insertion losses of the Tx portions must be as small as possible, the attenuation levels at harmonic frequencies must be 30-35 dB. Particularly for the EGSM-Tx portion where twice the transmitted frequency, 2fT(EGSM) overlaps the DCS received frequency, fR(DCS), the attenuation levels must be 35-40 dB. These required characteristics are shown in Fig. 4 taking EGSM as an example.

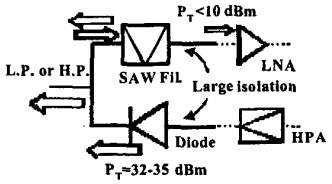

Fig. 5 Switch-less structure for Rx portions. SAW filter and pin diode are directly connected in parallel.

III. NEW RECEIVER PORTIONS INCLUDING SAW FILTERS

To simplify the circuits for Rx portions, we have proposed a new switch-less structure as shown in Fig. 5. The maximum power input to conventional LNAs in the off-state must be smaller than 10 dBm, which requires the isolation characteristics of over 25 dB at fTs between the output ports of the HPA and the input ports of LNAs. We have achieved the almost all required isolation level only by SAW filters using the previously developed SAW-resonator-coupled filter [12], i.e. one of a ladder-type configuration as shown in Fig. 6(a). While keeping low-loss characteristics, we can design very sharp cut-off frequency responses by combining electrically-connected multi-IDT resonators as shown in Fig. 6(b). This is very important because both EGSM and DCS have very wide bandwidths for the transmitted frequencies, fTs, and the received frequencies, fRs, but the relative spacing bandwidths between them are very narrow as shown in Fig. 2(a).

We have developed a direct-parallel connection between SAW filters and the switching pin diode as shown in Fig. 5, eliminating the need for pin diodes from Rx portions in the FEM as shown in Fig. 1(b). These parallel connections require SAW filters that have not only high attenuation levels but also high impedance characteristics at fTs. This is because to minimize the increase in the losses in the Tx portions due to the parallel connection, the

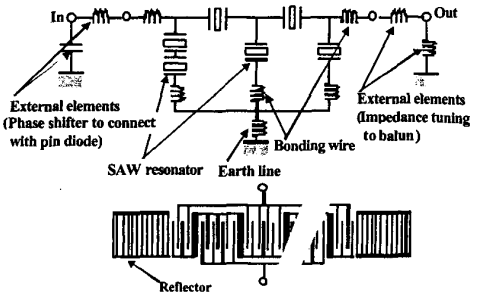

Fig. 6 Receiver SAW filter with high-power and sharp-cutoff frequency characteristics. (a) SAW-resonator-coupled filter, i.e. ladder-type configuration. (b) Electrically-connected multi-IDT SAW resonator.

input impedance of parallel-connected sides of the SAW filters must be designed as large as possible at fTs. Moreover, the SAW filters must have very-high-power handling capabilities and small non-linear characteristics to protect against the high transmitted power, i.e. 35 dBm and 32 dBm, entering from the Tx portions.

We achieved required characteristics by the previously published SAW-filter design procedures for the ladder-type configuration. The equivalent circuit is shown in Fig. 6(a), and SAW resonators are shown in Fig. 6(b) [12]. The external elements on the parallel-connected side act as a phase shifter and make the impedance of SAW filter as high as possible at fT. The role of external elements on the Rx side is impedance tuning to the balun. The electrically-connected multi-IDT SAW resonators have intrinsically high-power durability characteristics because of four-fold increased apertures compared with those of the conventional multi-finger IDT-type resonators with same impedance [12]. Furthermore, two SAW resonators connected serially are arranged as shunt-arm elements at the parallel-connected side within the filter of Fig. 6(a), which further increases power durability. We have already conducted power-accelerated aging test with input power of 10 watts at fT of EGSM and that of 5 watts at fT of DCS.

IV. EXPERIMENTAL RESULTS

We developed an FEM for use in an EGSM/DCS dual-band transceiver using DC demodulation. Ceramic multi-layered package as well as lumped-circuit elements were used. SAW chips were mounted in a pocket of the lower side on the package. About 70 % of circuits were made by lumped elements, i.e. miniature helical inductors and chip condensers mounted on the upper side of the package. We formed the remaining circuits using internal elements with thin ceramic layers. The baluns to transform the single-ended output port of the SAW filter into the differential output ports, were made of lumped elements. The size of the developed FEM was 8×8×1.85mm3. The control voltage and current value for switching were 2.5 V and about 6 mA, respectively for each pin diode in the on-state.

Frequency characteristics of the EGSM-Rx portion of the FEM, i.e. the characteristics from the antenna port to EGSM-Rx ports are shown in Figs. 7(a), (b) and (c). The antenna port has 50-Ω single-ended input impedance, while the Rx ports have 100-Ω differential output impedance between them. As shown in Figs. (a) and (b), the insertion loss was 3.0 dB, and sharp-cutoff frequency characteristics and sufficient attenuation levels against blockers were achieved. High suppression characteristics at harmonic frequencies over 35 dB were also obtained, which is peculiarly required for DC demodulation. Amplitude- and phase-imbalances less than ±0.4 dB and ±3°, respectively, are achieved as shown in Fig. (c). Recent RF-ICs using DC demodulation strongly require amplitude- and phase-imbalances less than ±1 dB and ±10°, respectively.

Frequency characteristics of the EGSM-Tx portion of the FEM, i.e. the characteristics from Tx port to the antenna port, are shown in Figs. 8(a) and (b), where both ports have the 50-Ω single-ended impedance. An insertion loss as small as 1.0 dB, and a suppression level over 35 dB at the 2nd- harmonic frequency were achieved. The suppression levels at the 3rd- and 4th-harmonic frequencies were over 30 dB.

Frequency characteristics of the DCS-Rx portion are shown in Figs. 9(a), (b) and (c), where the Rx ports also have 100-Ω differential output impedance. The insertion loss was 3.3 dB, and sufficient suppression levels against blockers were achieved. High suppression characteristics at harmonic frequencies over 35 dB were obtained. The amplitude- and phase-imbalances were less than ±0.5 dB and ±4°, respectively. The frequency characteristics of the DCS-Tx portion are shown in Figs. 10(a) and (b). The insertion loss is as small as 1.2 dB, and suppression levels at 2nd- and 3rd-harmonic frequencies are over 30 dB.

The isolation characteristics between Tx-input ports and Rx-output ports in EGSM- and DCS-Tx on-states are shown in Figs. 11(a) and (b), respectively. Isolation levels over 30 dB at fTs were achieved, which eliminates the need for pin diodes in the Rx portions of the FEM.

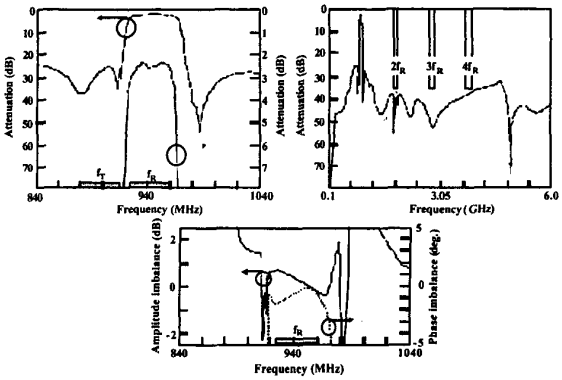

Fig. 7 Frequency characteristics for EGSM-Rx portion of FEM. (a) Pass-band characteristics. (b) Out-of-band characteristics. (c) Amplitude- and phase-imbalance characteristics.

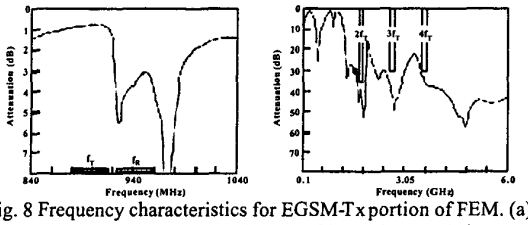

Fig. 8 Frequency characteristics for EGSM-Tx portion of FEM. (a) Pass-band characteristics. (b) Out-of-band characteristics.

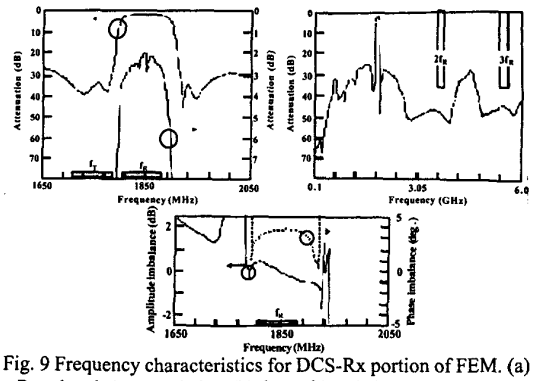

Fig. 9 Frequency characteristics for DCS-Rx portion of FEM. (a) Pass-band characteristics. (b) Out-of-band characteristics. (c) Amplitude- and phase-imbalance characteristics.

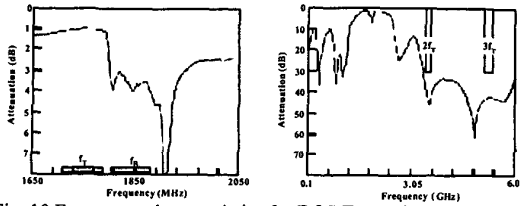

Fig. 10 Frequency characteristics for DCS-Tx portion of FEM. (a) Pass-band characteristics. (b) Out-of-band characteristics.

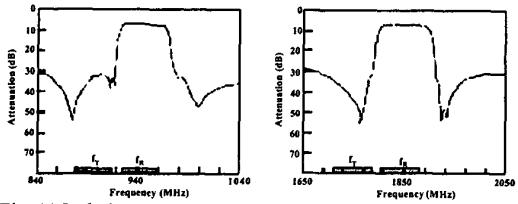

Fig. 11 Isolation characteristics between Tx-input ports and Rx-output ports of FEM in Tx on-state. (a) EGSM portion. (b) DCS portion.

V. FEMs FOR MULTI-BAND PHONES

In the near future, not only GSM/DCS/PCS triple-band phones but also EGSM/GSM850/DCS/PCS quad-band phones will be used in all over the world. The new invented configurations for the triple-band FEM is shown in Figs. 12. An example of the quad-band FEM will be also shown in another paper [13] The features of these configurations are as follows: (1) small numbers of pin diodes, (2) small numbers of control terminals and simple combination for control voltages, (3) possibility to reduce the size of FEMs, etc. These FEMs can be used with RF-ICs using DC demodulation.

VI. CONCLUSIONS

Assuming DC-demodulation method used in GSM-based multi-band cellular phones, required characteristics and new configurations for SAW FEMs were investigated. Design procedures and experimental results for new EGSM/DCS dual-band FEM were presented. Multi-band FEMs such as triple-band FEM and so on were also discussed.

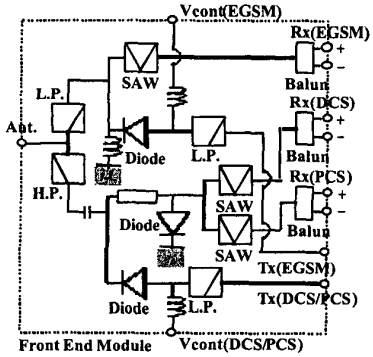

Fig. 12 Configurations of multi-band SAW FEMs. Example of triple-band FEM is shown.

VII. REFERENCES

[1] J. Strange and S. Atkinson, in IEEE Radio Frequency Integrated Circuits (RFIC) Symp. Proc., 2000, pp. 25-28.

[2] RF Transceiver IC for GSM900/1800 Dual Band Cellular systems, RF IC catalog of Hitachi Ltd., 2001.

[3] M. Hikita, N. Matsuura, N. Shibagaki, and K. Sakiyama, in IEEE Ultrason. Symp. Proc., 1999, pp. 385-388.

[4] N. Shibagaki, N. Matsuura, K. Sakiyama, and M. Hikita, in IEEE Ultrason. Symp. Proc., 2000, pp. 391-394.

[5] Document of 3rd Generation Partnership Project; Technical Specification Group GSM/EDGE (3GPP TS 05.05), V8.9, 2001-04.

[6] T. Watanabe, K. Furutani, N. Nakajima, and H. Mandai, in IEEE MTT-S Int. Microwave Symp. Digest, 1999, pp. 215-218.

[7] F. Uchikoba, T. Goi, N. Harada, and S. Nakai, in Proc. Int. Symp. on Acoustic wave Devices for Future Mobile Communication Systems, Mar. 2001, pp. 145-150.

[8] R. Lucero, W. Qutteneh, A. Pavio, D. Meyers, and J. Estes, in IEEE Radio Frequency Integrated Circuits (RFIC) Symp. Proc., 2001, pp. 213-216.

[9] T. Yamawaki, M. Kokubo, K. Irie, H. Matsui, K. Hori, T. Endou, H. Hagisawa, T. Furuya, Y. Shimizu, M. Katagishi, and J. R. Hildersley, IEEE J. Solid-State Circuits, vol. 32, pp. 2089-2096, 1997.

[10] Cover Feature, in Microwave Journal, Jan. 2001, pp. 200-214.

[11] MOS FET Power Amplifier Module for E-GSM and DCS 1800 Dual Band Handy Phone, Power Module catalog of Hitachi Ltd., 2000.

[12] M. Hikita, N. Shibagaki, K. Sakiyama, and K. Hasegawa, IEEE Trans. Ultrason., Ferroelect., Freq. Contr., vol. 42, pp. 495-508, 1995.

[13] M. Hikita, et al, to be published in IEEE Ultrason. Symp. Proc., 2002.